This is a "preproof" accepted article for *Animal Nutriomics*.
This version may be subject to change during the production process.
10.1017/anr.2025.3

The probiotic characteristics of *Lactobacillus reuteri* ZJ617and its resistance to *Escherichia coli* O157:H7 challenge in HFD-fed mice

Yanfei Ma[1], Yingying Mao[1], Zhaoxi Deng[1], Shanshan Wang[1], Jingliang Liu[1] and Haifeng Wang[1] *

[1] College of Animal Sciences, Zhejiang University, The Key Laboratory of Molecular Animal Nutrition, Ministry of Education, Hangzhou, 310058, China.

*Corresponding author. E-mail: haifengwang@zju.edu.cn (H.W.)

Abstract

A high-fat diet increases susceptibility to *Escherichia coli* colonization in the intestine and raises the risk of intestinal diseases. *Lactobacillus reuteri*, a commensal bacterium, plays a crucial role in regulating intestinal function and maintaining immune homeostasis. In this study, we aimed to evaluate the effects of *L. reuteri* on gut barrier function and systemic inflammation in HFD-fed mice challenged with Shiga toxin-producing *E coli* O157:H7, and to further elucidate the potential protective mechanisms involved. The results show that supplementation of *L. reuteri* ZJ617 mitigates intestinal barrier impairment, inflammatory cell infiltration and systemic inflammation induced by *E. coli* O157:H7. The potential mechanisms of *L. reuteri* ZJ617 deal with it involving in forming biofilm, producing functional amino acids and various secondary metabolites. Our works provided comprehensively analysis of potential properties of *L. reuteri* ZJ617 and indicated that *L. reuteri* ZJ617 is a promising probiotic to prevent *E. coli* O157:H7 infection.

This is an Open Access article, distributed under the terms of the Creative Commons Attribution-NonCommercial-NoDerivatives licence (http://creativecommons.org/licenses/by-nc-nd/4.0), which permits non-commercial re-use, distribution, and reproduction in any medium, provided that no alterations are made and the original article is properly cited. The written permission of Cambridge University Press must be obtained prior to any commercial use and/or adaptation of the article.

Downloaded from https://www.cambridge.org/core. 07 Feb 2025 at 10:21:54, subject to the Cambridge Core terms of use.

Keywords: *Lactobacillus reuteri*, intestinal barrier, high-fat diet, mice

Introduction

A high-fat diet is an environmental risk factor associated with increase for intestinal inflamatory[1-3]. This is due to high-fat diet-induced impairments in mitochondrial bioenergetics, which exacerbate epithelial hypoxia to support the proliferation of *Escherichia coli* and other *Enterobacteriaceae*[4-5]. These pathogenic bacteria further accelerate the risk of intestinal barrier impairment, mucosal infections and systemic inflammation[6-7], posing a threat to both human and animal intestinal health.

Probiotics, as live microbial food components, are recognized for their beneficial effects on animal and human health. *L. reuteri* strains are part of commensal microbiota in the intestines of piglets and play important roles in microbiota maturation[8] and physical function regulation[9]. Previous studies found that *L. reuteri* produce lactic acid[10], reutericyclin[11] and exopolysaccharides[12], exhibiting antibacterial properties against certain intestinal pathogens in *vitro*[12-15]. The intestinal mucosa functions as a conduit for absorbing food-derived nutrients and microbiome-derived metabolites, while also acting as a barrier to prevent microbial invasion and regulate inflammatory responses to the diverse contents of the lumen. *L. reuteri* has been shown to repair gut damage and alleviate intestinal inflammation after *E. coli* K88 infection[16-17]. However, few studies have evaluated the effects of *L. reuteri* on gut barrier function and systemic inflammation in HFD-fed individuals exposed to pathogenic bacteria, nor have the illustrate the potential protective mechanism involved.

In previous studies, we isolated and cultured a high adhesive *L. reuteri* ZJ617 from piglet intestines[18], which demonstrated the ability to regulate intestinal barrier and reduce inflammatory in piglet or mouse model challenged with lipopolysaccharide under a normal diet[19-20]. In the current study, we used Shiga-toxin-producing *E. coli* O157:H7 as a challenge for HFD-fed mice, a well-known zoonotic pathogen that cause gastroenteritis. Through combined complete genome sequencing, metabolomics, and functional prediction of microorganisms, we aimed to explore the mechanism by which *L. reuteri* ZJ617 mitigates *E. coli* O157:H7 infection-induced intestinal barrier impairment and systemic inflammatory in obese mice.

Downloaded from https://www.cambridge.org/core. 07 Feb 2025 at 10:21:54, subject to the Cambridge Core terms of use.

Materials and Methods

Animals and experiment design

Four-week-old male C57BL/6J mice, specific pathogen-free (SPF), were purchased from Shanghai SLAC Laboratory Animal Co., Ltd. (Shanghai, China). Prior to the experiment, the mice were acclimatized to the environment (23±1 ℃, 12-h light-dark cycle) with unrestricted access to food and drinking water for one week. Following acclimation, the mice were randomly assigned into two groups: HFD (High fat diet, containing 60% kcal from fat; PD6001) (n=18) and HFD supplement with *L. reuteri* ZJ617 (n=9, one of which died unexpectedly). The mice were maintained on an HFD for 14 weeks. 2 days before being sacrificed, half of the HFD mice and all HFD mice supplemented with *L. reuteri* ZJ617 were challenged with 200 μL *E. coli* O157:H7 (10^9 cfu/mL) for 48 hours. All diets were sourced from Changzhou SYSE Bio-Tec. Co., Ltd. (Changzhou, China). Animal experiments were conducted in accordance with the "Regulation for the Use of Experimental Animals" of Zhejiang Province, China and approved by the Animal Care and Use Committee of Zhejiang University (ETHICS CODE Permit no. ZJU20240770).

L. reuteri ZJ617 had previously been isolated from piglet small intestines and stored in 20% glycerol at -80℃ until usage. The strain was anaerobically cultured in sterilized De MRS medium at 37℃ for 18 hours. The final concentration of *L. reuteri* ZJ617 used was 10^9 cfu/mL in drinking water. The drinking water was refreshed every day.

Serum biochemical analysis

Blood samples were centrifuged at 3000 g for 15 min at 4℃ to produce serum samples. The levels of serum IL-1β , TNF-α and endotoxin were determined using corresponding assay kits (H002-1-2, H052-1-1 and A054-1-1, respectively; Nanjing Jiancheng Bioengineering Institute, Nanjing, China). All processes were performed according to manufacturer's instructions.

Histological analysis

After euthanasia, the ileum and colon of the mice were preserved in 4% paraformaldehyde (4% PFA). The fixed, paraffin-embedded samples sections were stained with hematoxylin and eosin (H&E) to evaluate the villus height and crypt depth of ileum or colon, respectively, followed by microscopical examination. All processes were carried out according to manufacturer's instructions. The intestinal villus height and crypt depth were quantified using Image J.

Downloaded from https://www.cambridge.org/core. 07 Feb 2025 at 10:21:54, subject to the Cambridge Core terms of use.

Alcian blue staining

The above fixed paraffin-embedded colon samples sections were stained with alcian blue to assess mucus secretion of colon[21], according to manufacturer's instructions. Then the samples under glass slide were observed with a microscope. The Image J was applied to quantify the mucus secretion.

Western blotting

Ileum tissue were lysed in RIPA buffer supplemented with PMSF, proteinase inhibitor and phosphatase inhibitors (Beyotime Technology, Shanghai, China) while kept on ice. The lysates were then centrifuged at 12,000 rpm for 10 minutes. The supernatant was collected, denatured in sample buffer, and separated using SDS-PAGE. Samples were transferred onto PVDF membranes with a pore size of 0.45 μM. For proteins detection, the following primary antibodies were used at a 1:1000 dilution: ZO-1 (Abcam, ab276131), occludin (Abcam, ab216327) and β-actin (Cell Signaling Technology, 4970). Visualization of proteins was performed on film using horseradish peroxidase–conjugated secondary antibodies diluted at 1:5000.

16S rRNA amplicon sequencing

Microbial DNA was extracted from intestinal contents, and the total DNA was quantified by Nanodrop 2000 (Thermo Fisher, USA). The V3-V4 region of the bacteria 16S rRNA genes were amplified with primers 341F 5'-CCTACGGGRSGCAGCAG-3' and 806R 5'-GGACTACVVGGGTATCTAATC-3'[22]. PCRs were conducted, and the library was created using Qubit. The purified amplicons were combined in equal amounts and sequenced in paired-end on an Illumina MiSeq PE250 platform (Illumina, San Diego, USA) following the manufacturer's protocols. Raw reads were first removed barcode to generate high-quality reads, and then were assembled. ASVs were identified and generated through standard clustering at 100% similarity using Deblur. Each representative sequence was classified to a taxon with the RDP Classifier. ASV profiling was carried out with QIIME2. Based on the ASV table, a Venn diagram was used to visualize common and unique features between the three groups. Alpha diversity was evaluated using chao1 and the corresponding significance was determined using the Kruskal-Wallis test. Beta diversity was estimated using principal coordinate analysis (PCoA) on an unweighted unifrac distance matrix using QIIME2 software. QIIME2 was utilized for calculating each species abundance and taxonomic distributions across different levels.

Downloaded from https://www.cambridge.org/core. 07 Feb 2025 at 10:21:54, subject to the Cambridge Core terms of use.

Co-occurrence network analysis

Based on the genus abundances, Spearman's rank correlation analysis was performed to identify the differences among the different group. Data with a correlation coefficient $|\rho$-value$|$ >0.5 and a *P*-value <0.01 were selected to construct a co-occurrence network. Network graphs and indices, such as average degree and average clustering coefficient, were displayed and calculated using the Cytoscape software (3.9.0).

PICRUSt2 for prediction of metagenome functions

PICRUSt2 was utilized to predict metagenome functions[23]. KEGG (Kyoto Encyclopedia of Gene and Genomes) was used to support pathway profiles. All predicted pathways were obtained using a Wilcoxon-test.

Scanning electron microscope

L. reuteri ZJ617 was anaerobically cultured in sterilized De Man Rogosa and Sharpe (MRS) medium at 37℃. After 18 h cultured, the supernatant was removed, and the bacteria were washed three times with PBS. Then the bacteria were preserved in 2.5% glutaraldehyde for more than 4 h and then were post-fixed with 1% OsO4 for 1 h. After dehydration with ethanol, the samples were dried with a critical point dryer, the sections were observed with a scanning electron microscope (Hitachi SU-8010). All processes were performed according to the instructions of the Bio-ultrastructure analysis Laboratory of Analysis center of Agrobiology and environmental sciences, Zhejiang University.

DNA extraction and genome sequencing, assembly and annotation

L.reuteri ZJ617 genomic DNA was extracted according to manufacturer's instructions. The DNA quantity and quality were tested by the NanoDrop 2000 (Thermo Fisher Scientific), and then the qualitied DNA was further purified. The whole genome was sequenced using the Pacific Biosciences platform and the Illumina NovaSeq 6000 platform. Quality control was performed by using Trimmonmatic[24]. All good qualitied data were assembled using ABySS software[25]. The gene function annotation using various databases, including NR (Non-Redundant Protein database), Swiss-Prot (http://uniprot.org), KEGG (Kyoto Encyclopedia of Gene and Genomes), GO (Gene Ontology), COG (Clusters of Orthologous Groups), CAZy (Carbohydrate-Active EnZymes Database), CARD (The Comprehensive Antibiotic Resistance Database), TCDB (Transporter Classification Database), PHI (Pathogen Host Interactions), VFDB (Virulence Factors of Pathogenic Bacteria).

Downloaded from https://www.cambridge.org/core. 07 Feb 2025 at 10:21:54, subject to the Cambridge Core terms of use.

The anti-SMASH analysis

To understand the secondary metabolites production capacities of *L.reuteri* ZJ617, assembled genome was analyzed for the presence of secondary metabolite biosynthetic gene clusters (BGCs) using anti-SMASH 7.0[26]. MiBiG database was applied to identify both known and putatively novel BGCs that may be involved in the biosynthesis of major compound classes, such as polyketides, terpenoids, non-ribosomal peptides (NRPs), and beta-lactones[27].

Metabolomic profiling

After 18 h of culture, the bacteria were removed, and supernatant was harvested. The metabolites were analyzed by liquid chromatography time-of-flight mass spectrometer (LC-TOF-MS). Briefly, adding 1.2 mL methanol to 300 μL culture medium and vortex for a while. Incubating the mixture on ice for 30 min and centrifuging 15000g at 4℃ for 15 min. Transfer 1.2 mL supernatant for a new clean tube and re-centrifuge for once. Transfer 900 μl supernatant into two aliquots and dry with freeze dryer. After drying, resolving the aliquot with 150 μl 60% acetonitrile, and incubating on the ice for 3 min and centrifuge 15000 g at 4℃ for 15 min. Then transfer supernatant for a new clean tube and re-centrifuge for once. The supernatant was filtered with a nylon filter and injected onto the LC-TOF-MS system for detection and analysis.

For the data of the metabolites of intestinal contents, the abundance differences were obtained using a student t-test with Benjamini-Hochberg's method corrected *P*-values. Differential metabolites were defined as those with variable importance in the projection (VIP) >1.0 obtained from PLS-DA, $|\mathrm{Log_2}\,(\mathrm{Foldchange})|>1$ and $P < 0.05$.

Statistical analysis

A one-way analysis variance (ANOVA) was performed for identify the differences in animal study, followed by Dunnett tests. All data are shown as means ± SD. Statistical analyses were performed using GraphPad Prism (USA). $P < 0.05$ was considered statistically significant.

Results

Functional annotation of complete genome unravels probiotic characteristics of *L. reuteri* ZJ617

Scanning electron microscope images show that *L. reuteri* ZJ617 was rod-like with secretions on its surface (Fig. 1). Then, we conducted a genomic analysis to obtain a comprehensive understanding of the potential probiotic characteristics of *L. reuteri* ZJ617. The strain contains a

Downloaded from https://www.cambridge.org/core. 07 Feb 2025 at 10:21:54, subject to the Cambridge Core terms of use.

single circular chromosome of 2,538,072 bp and two plasmids (plasmid 1:143, 069 bp; plasmid 2:14, 763 bp) with 38.33% in average GC content (Fig. 2A). The various genes coding for acid tolerance, bile tolerance, adhesion and biofilm formation was presented in genome of *L. reuteri* ZJ617 (Table S1). Furthermore, annotation of KEGG database showed that metabolic pathway is the dominant functional pathway, and approximately 12.9% (150 genes) were classified into biosynthesis of secondary metabolites in the top functional pathways (Fig. 2B). Notably, the genome of *L. reuteri* ZJ617 has a set of genes involved in the de novo synthesis two of essential amino acids for animal production, including Threonine and L-lysine (Fig. 2C). In addition, the anti-SMASH analysis predicted the type III polyketide synthase (T3PKS) is the single secondary metabolite biosynthetic gene clusters (BGCs) (Fig. 2D). The MIBIG algorithm grouped the BGCs predicted by anti-SMASH into 280 gene cluster families (GCFs), with 141 Polyketide、41 NRP, 61 NRP-Polyketide, 20 Terpene, 7 Saccharide, 6 Alkaloid and 4 ribosomally synthesized and post-translationally modified peptide (RiPPs) (Fig. 2E).

Metabolomics analysis metabolites of *L. reuteri* ZJ617

We next performed an untargeted metabolomic profiling on probiotic-cultured supernatant to further identify metabolic patterns of *L. reuteri* ZJ617. The partial least squares discriminant analysis (PLS-DA) showed a significant change of metabolites before and after culture (Fig. 3A). A total of 788 metabolites were detected in the supernatant, among which 99 were down-regulated and 135 were up-regulated relative to those in the MRS medium (Fig. 3B). These metabolites were further divided into primary metabolites and secondary metabolites (Fig. 3C). Amino acids, peptides, and analogues are the dominant up-regulated metabolites (Fig. S1). The KEGG pathway enrichment analysis also suggested that *L. reuteri* ZJ617 is mainly responsible for amino acid metabolism (Fig. 3D). Consistence with genomic information, the L-threonine and lysine were detected, as well as their precursor (L-homoserine) (Fig. 3E). For the secondary metabolites, ursodeoxycholic acid, gallate, trans-2-hydroxycinnamate, trans-3-hydroxycinnamate and cis-2-hydroxycinnamate were significantly up-regulated in the supernatant (Fig. 3F).

***L. reuteri* ZJ617 prevents obese mice from *E. coli* O157:H7-induced serum inflammation**

The experimental design and workflow are shown in Fig. 4A. HFD mice challenged with *E. coli* O157:H7 for 48 h experienced a slight decline in body weight, however, supplementation

Downloaded from https://www.cambridge.org/core. 07 Feb 2025 at 10:21:54, subject to the Cambridge Core terms of use.

with *L. reuteri* ZJ617 contributed to maintaining their weight (Fig. 4B). There is no significant difference in serum IL-1β, TNF-α and endotoxin between HFD and HE mice, and pretreated with *L. reuteri* ZJ617 significantly decrease the serum inflammation (Fig. 4C-4E).

L. reuteri ZJ617 attenuates obese mice from _E. coli_ O157:H7-induced intestinal barrier damages

As shown in pathological section, there is inflammatory cell infiltration in the ileum and colon tissues of HFD-fed mice both before and after *E. coli* O157:H7 challenge (Fig. 5A and 5B). However, supplementation with *L. reuteri* ZJ617 provides protection against this infiltration (Fig. 5A and 5B). Additionally, there is no significant difference in villus height, crypt depth, and the ratio of villus height to crypt depth in HFD and HE mice (Fig. 5A and 5B). Regarding the intestinal barriers in the colon, *E. coli* O157:H7 challenge did not affect mucus secretion in HFD mice (Fig. 5C), but significantly down-regulated the expression of zonula occludens1 (ZO-1) (Fig. 5D) and caused a numerical decline in occludin (Fig. 5E). Notably, compared with the HE mice, *L. reuteri* ZJ617 supplementation significantly increased villus height and the ratio of villus height to crypt depth, promoted mucus secretion, and up-regulated colon tight junction protein ZO-1 and occludin (P=0.08) (Fig. 5A-5E).

L. reuteri ZJ617 induces alterations in gut microbiome structure and functions

To evaluate the impacts of *L. reuteri* ZJ617 on the gut microbiota, we performed 16S ribosomal RNA gene amplicon sequencing on intestinal contents from three groups. Venn diagram showed common and unique features between three groups, from which 32, 30 and 23 unique features in the HFD, HE and HZE mice, respectively (Fig. 6A). Chao1 indices supported that *E. coli* O157:H7 infection significantly increased the diversity of the microbiota in HFD-fed mice (Fig. 6B), whereas no difference was found between HFD mice and HZE mice (Fig. 6B), suggesting that *L. reuteri* ZJ617 supplementation stabilized microbial diversity. The unweighted UniFrac-based principal coordinates analysis (PCoA) revealed a clear clustering of the gut microbiota for each group (ANOSIM, P=0.002) (Fig. 6C). Additionally, the *E. coli* O157:H7 challenge decreased the relative abundance of *Romboutsia*, *Enterothabdus*, *Lactobacillus* and *Dubosiella* compared to HFD mice. However, *L. reuteri* ZJ617 supplementation prevented them decreased (Fig. 6D).

Large modules (more than 3 nodes) within the HFD, HE and HZE networks were identified

Downloaded from https://www.cambridge.org/core. 07 Feb 2025 at 10:21:54, subject to the Cambridge Core terms of use.

by focusing on the relevance of genera and the proportion of major phyla to uncover potential changes in gut microbial interactions following *L. reuteri* ZJ617 supplementation. The HFD mice exhibited compact and larger networks featured with many more nodes (55) and edges (105) (Fig. 6E). In contrast, *E. coli* O157:H7 challenge led to looser and smaller networks, with fewer nodes (40) and edges (37) (Fig. 6F). HE mice (27.03%) showed a lower ratio of positive correlations compared to HFD mice (72.97%) (Table S2), indicating that bacteria genera in HE mice tended to co-exclude (negative correlation) rather than co-occur (positive correlation). However, the number of negative edges is not reduced (Table S2). Furthermore, the reduced average degree (Fig. 6H) and average clustering coefficient (Fig. 6I) in HFD mice challenged with *E. coli* O157:H7 reflected an impaired network complexity. Of note, pre-treatment with *L. reuteri* ZJ617 prevented the reduction in nodes, percentage of positive edges, degree, and clustering coefficient, as well as the loosening of the network (Fig. 6G-6I).

We applied PICRUSt2 to predict metagenome functions between HE and HZE mice. Among the 414 identified pathways, a total of 66 differential pathways were changed by *L. reuteri* ZJ617 supplementation, like preventing L-lysine, L-tryptophan, gallate, hydroxycinnamate degradation, reducing LPS biosynthesis and other functional pathways (Fig. 6J).

Discussion

A high-fat diet favors the emergence of *E. coli* in the ileal, cecal and colonic mucosa, thereby increasing host susceptibility to chronic inflammatory bowel disease. This dietary pattern further supports *E. coli* colonization or enhances the risk or chemically induced colitis[28-29]. Here, we found that *E. coli* O157:H7 challenge exhibited an increased serum inflammatory factors compared to sole HFD-fed mice, although the increase was not statistically significant. One possible reason is that wild-type C57BL/6J mice do not exhibit a strong genetic predisposition to bacterial infection[29]. Additionally, the high-fat diet compromises the intestinal barrier function, and creates a low-grade inflammation environment in the host[30], which may have masked the incremental effect of *E. coli* O157:H7 infection on serum inflammatory markers. Pretreatment with *L. reuteri* ZJ617 significantly up-regulated intestinal tight junction proteins and promotes mucin secretion, both of which may contribute to its protective effect against intestinal and systemic inflammation induced by HFD, while also enhancing resistance to subsequent *E. coli* O157:H7 challenge.

Downloaded from https://www.cambridge.org/core. 07 Feb 2025 at 10:21:54, subject to the Cambridge Core terms of use.

Probiotic biofilms can resist pathogen colonization in the gut by occupying ecological niches[31]. The genomic traits of *L. reuteri* ZJ617 reveal numerous factors for acid and bile tolerance, which consistent with our previous obtained phenotypic traits[18]. The ability of probiotics to colonize and survives in the gastrointestinal tract by resisting acidic and bile conditions is the very first step in exerting their antibacterial effects. Notably, these resistances are believed to be partially dependent on their ability to form biofilms[32]. Studies have indicated that the formation of biofilm by *L. reuteri* reduced *E,coli* O157:H7 survive in *vitro*[33]. *L. reuteri* ZJ617 encodes both of genes related to EPS biosynthesis and LuxS, which are considerate to involved in biofilm formation[34-35], and has been demonstrated to have an inhibition effect on *E. coli* O157:H7[36-38]. Therefore, the ability of *L. reuteri* ZJ617 to form solid biofilm is one of factor to control pathogen infection.

Consistent with the other strains of *L. reuteri* derived from bovine or murine[11, 39], the genome of *L. reuteri* ZJ617 also participates in multiple amino acids biosynthesis pathways. In *vivo*, the microbiome function prediction suggested that supplementation with *L. reuteri* ZJ617 may prevent lysine degradation. This phenomenon might be contributed to the potential of *L. reuteri* ZJ617 to produce lysine as indicated by its metabolic profile, which has been confirmed to be beneficial for modulating immune tolerance in colitis[40]. Another study showed that high dietary ration of lysine could increase the gene expression of tight junction proteins in *Clostridium perfringens*-challenged turkeys[41]. In addition, the microbial prediction suggests that *E. coli* O157:H7 challenged accelerate L-tryptophan degradation, which is consistent with phenomenon in DSS-induced Ulcerative colitis[42]. Conversely, *L. reuteri* ZJ617 can prevent it, which may result in more L-tryptophan accumulate in intestine. Numerous studies have reported that *L. reuteri* can convert tryptophan into indole derivatives to regulate host immune [43-44]. Among these derivatives, indole-3-propionic acid has been shown to enhance intestinal barrier function by promoting the expression of tight junction proteins and upregulating the expression of mucins such as MUC2 and MUC4.[45]. Furthermore, both the genomic information and metabolic profile of *L. reuteri* ZJ617 monocultures revealed an increase of L-threonine production, which has an ability to optimize intestinal barrier function[46-47]. Therefore, the amino acids derived from *L. reuteri* ZJ617 or its influenced microbiome may serve as one contributor to mitigate *E. coli* O157:H7-induced inflammatory and gut barrier impairment. Furthermore, lysine, threonine and tryptophan produced

Downloaded from https://www.cambridge.org/core. 07 Feb 2025 at 10:21:54, subject to the Cambridge Core terms of use.

by *L. reuteri* ZJ617, as essential nutrients, may not only serve as immunoregulators, but also support the growth and development of various organism, including microorganisms, animals and humans.

Microbial secondary metabolites and their active compounds are another considerable antibacterial candidate, which has been extensively reported in recent study[48-49]. Although our previous study and others have reported that the supernatant of *L. reuteri* monocultures play important roles in protecting from pathogen, regulating intestinal barrier and inflammatory[50-51], few studies have explored and discussed the compositions and potential functions of *Lactobacillus*-derived secondary metabolites. The genomic information shows that *L. reuteri* ZJ617 is mainly involved in biosynthesis of polyketide, a common characteristic observed in *L. reuteri* as confirmed by other studies[52]. We also detected an increase of hydroxycinnamate, one of polyketide, in supernatant after monocultures. Interestingly, previous study has demonstrated this polyketide compound can protect against LPS-induced intestinal epithelial cells injury[53]. And its methyl ester derivative, methyl p-hydroxycinnamate, has an same anti-inflammatory effects in RAW264.7 cells challenged with LPS[54]. The possible mechanism may involve in *L. reuteri* derived polyketide activate the aryl hydrocarbon receptor[52], which is a potential target for the control of intestinal inflammation[55-56]. In addition, *L. reuteri* ZJ617 can produce other secondary metabolites, like gallate (Benzonoids) and ursodeoxycholic acid (terpenoids), which have been confirmed to be beneficial for protecting from pathogeny infection, alleviating intestinal barrier dysfunction and related inflammation[57-60]. Given the antibacterial properties of secondary metabolites, *L. reuteri* ZJ617 may have the potential to replace antibiotics in treating diseases caused by pathogenic infections in animal production or human therapy.

Since *L. reuteri* ZJ617 produces numerous metabolites, which serve as interactive mediators for complex inter-microbial communication[61]. The cooperating networks of gut microbes are considered metabolically efficient[62]. This means that one bacterium provides nutrients for another, supporting its survival and colonization. Conversely, competitive relationships are believed to stabilize microbial structure[62]. This is supposed as a rescue measure, where adaptive immunity helps reestablish a healthy microbiome by suppressing species whose existence is causing harm during pathogen infection[63-64]. Indeed, we observed that *E. coli* O157:H7 challenge shifted microbial networks in HFD mice by reducing the positive links while maintaining the number of

Downloaded from https://www.cambridge.org/core. 07 Feb 2025 at 10:21:54, subject to the Cambridge Core terms of use.

negative links, which suggesting that *E. coli* O157:H7 disrupts the metabolic efficiency of the gut microbiome, and attempts to stabilize microbial structure to exert health benefits to host. Major alteration of microbial community composition is often associated with ill conditions. One supposed that the disturbed microbial structure leads to an increase in LPS release[65]. Correspondingly, pretreated with *L. reuteri* ZJ617 remain maintain complicated and balanced networks. The microbiome prediction showed that *L. reuteri* ZJ617 reduced LPS biosynthesis from bacteria. Long term consumption of a high-fat diet decreases goblet cell numbers, impairs mucus secretion and compromises gut barrier integrity both in small intestine and colon, leading to increased LPS translocation into the bloodstream, contributing to systemic inflammation[66], which is consistent with the phenomenon we detected in serum of HE mice. However, supplementation with *L. reuteri* ZJ617 appears to promote mucus production and reduce the level of serum inflammatory factors. In addition, the mucus layer covering the intestinal surface effectively keeps the majority of gut bacteria at a safe distance from the epithelial cells lining the intestine[67], which is may another potential approach to defend against *E. coli* O157:H7 challenge.

In summary, our study found that *L. reuteri* ZJ617 alleviates gut barrier injury, intestinal inflammatory cell infiltration and systemic inflammatory induced by *E. coli* O157:H7 in HFD mice. We comprehensively analyzed the possible mechanisms involved, including the properties of biofilm, amino acids and secondary metabolites biosynthesized by *L. reuteri* ZJ617 and balanced microbiome. In the future, specific functional metabolites need to be identified and studied for their precise contributions, as well as their mechanism in preventing *E. coli* O157:H7 infection.

Acknowledgements

We specially thank professor Yizhen Wang from College of Animal Sciences, Zhejiang University for providing the *E. coli* O157:H7.

Funding

This study was supported by grants from the Key R & D Projects of Zhejiang Province (2022C04034; 2022C02015).

Author contributions

Y.M. and H.W. planned the project and the experiments. Y.M. analyzed the data; Y.M., Y.M., Z.D., S.W., J.L. performed the experiments; Y.M., and H.W. wrote the original draft; Y.M. and H.W.

Downloaded from https://www.cambridge.org/core. 07 Feb 2025 at 10:21:54, subject to the Cambridge Core terms of use.

were responsible for writing review and editing. Funding acquisition was the responsibility of H.W.

Competing Interests

The authors declare no competing interests.

Reference

1. Gruber, L.; Kisling, S.; Lichti, P.; Martin, F. P.; May, S.; Klingenspor, M.; Lichtenegger, M.; Rychlik, M.; Haller, D., High fat diet accelerates pathogenesis of murine Crohn's disease-like ileitis independently of obesity. *PLoS One* **2013,** *8* (8), e71661.
2. Paik, J.; Fierce, Y.; Treuting, P. M.; Brabb, T.; Maggio-Price, L., High-fat diet-induced obesity exacerbates inflammatory bowel disease in genetically susceptible Mdr1a-/- male mice. *J Nutr* **2013,** *143* (8), 1240-7.
3. Xie, R.; Sun, Y.; Wu, J.; Huang, S.; Jin, G.; Guo, Z.; Zhang, Y.; Liu, T.; Liu, X.; Cao, X.; Wang, B.; Cao, H., Maternal High Fat Diet Alters Gut Microbiota of Offspring and Exacerbates DSS-Induced Colitis in Adulthood. *Front. Immunol.* **2018,** *9*, 2608.
4. Yoo, W.; Zieba, J. K.; Foegeding, N. J.; Torres, T. P.; Shelton, C. D.; Shealy, N. G.; Byndloss, A. J.; Cevallos, S. A.; Gertz, E.; Tiffany, C. R.; Thomas, J. D.; Litvak, Y.; Nguyen, H.; Olsan, E. E.; Bennett, B. J.; Rathmell, J. C.; Major, A. S.; Bäumler, A. J.; Byndloss, M. X., High-fat diet-induced colonocyte dysfunction escalates microbiota-derived trimethylamine N-oxide. *Science* **2021,** *373* (6556), 813-818.
5. Lee, J. Y.; Cevallos, S. A.; Byndloss, M. X.; Tiffany, C. R.; Olsan, E. E.; Butler, B. P.; Young, B. M.; Rogers, A. W. L.; Nguyen, H.; Kim, K.; Choi, S. W.; Bae, E.; Lee, J. H.; Min, U. G.; Lee, D. C.; Bäumler, A. J., High-Fat Diet and Antibiotics Cooperatively Impair Mitochondrial Bioenergetics to Trigger Dysbiosis that Exacerbates Pre-inflammatory Bowel Disease. *Cell Host Microbe* **2020,** *28* (2), 273-284.e6.
6. Thaiss, C. A.; Levy, M.; Grosheva, I.; Zheng, D.; Soffer, E.; Blacher, E.; Braverman, S.; Tengeler, A. C.; Barak, O.; Elazar, M.; Ben-Zeev, R.; Lehavi-Regev, D.; Katz, M. N.; Pevsner-Fischer, M.; Gertler, A.; Halpern, Z.; Harmelin, A.; Aamar, S.; Serradas, P.; Grosfeld, A.; Shapiro, H.; Geiger, B.; Elinav, E., Hyperglycemia drives intestinal barrier dysfunction and risk for enteric infection. *Science* **2018,** *359* (6382), 1376-1383.
7. Genser, L.; Aguanno, D.; Soula, H. A.; Dong, L.; Trystram, L.; Assmann, K.; Salem, J. E.; Vaillant, J. C.; Oppert, J. M.; Laugerette, F.; Michalski, M. C.; Wind, P.; Rousset, M.; Brot-Laroche, E.; Leturque, A.; Clément, K.; Thenet, S.; Poitou, C., Increased jejunal permeability in human obesity is revealed by a lipid challenge and is linked to inflammation and type 2 diabetes. *J Pathol* **2018,** *246* (2), 217-230.
8. Wang, G.; Wang, X.; Ma, Y.; Cai, S.; Yang, L.; Fan, Y.; Zeng, X.; Qiao, S., Lactobacillus reuteri improves the development and maturation of fecal microbiota in piglets through mother-to-infant microbe and metabolite vertical transmission. *Microbiome* **2022,** *10* (1), 211.
9. Lin, Z.; Wu, J.; Wang, J.; Levesque, C. L.; Ma, X., Dietary Lactobacillus reuteri prevent from inflammation mediated apoptosis of liver via improving intestinal microbiota and bile acid metabolism. *Food Chem.* **2023,** *404* (Pt B), 134643.

Downloaded from https://www.cambridge.org/core. 07 Feb 2025 at 10:21:54, subject to the Cambridge Core terms of use.

10. Behare, P. V.; Ali, S. A.; Mishra, V. S. N.; Gómez-Mascaraque, L. G.; McAuliffe, O., Fructose-induced topographical changes in fructophilic, pseudofructophilic and non-fructophilic lactic acid bacterial strains with genomic comparison. *World J Microbiol Biotechnol* **2023,** *39* (3), 73.

11. Huang, K.; Shi, W.; Yang, B.; Wang, J., The probiotic and immunomodulation effects of Limosilactobacillus reuteri RGW1 isolated from calf feces. *Front Cell Infect Microbiol* **2022,** *12*, 1086861.

12. Kšonžeková, P.; Bystrický, P.; Vlčková, S.; Pätoprstý, V.; Pulzová, L.; Mudroňová, D.; Kubašková, T.; Csank, T.; Tkáčiková, Ľ., Exopolysaccharides of Lactobacillus reuteri: Their influence on adherence of E. coli to epithelial cells and inflammatory response. *Carbohydr. Polym.* **2016,** *141*, 10-9.

13. Al-Nabulsi, A. A.; Osaili, T. M.; Oqdeh, S. B.; Olaimat, A. N.; Jaradat, Z. W.; Ayyash, M.; Holley, R. A., Antagonistic effects of Lactobacillus reuteri against Escherichia coli O157:H7 in white-brined cheese under different storage conditions. *J Dairy Sci* **2021,** *104* (3), 2719-2734.

14. Muthukumarasamy, P.; Han, J. H.; Holley, R. A., Bactericidal effects of Lactobacillus reuteri and allyl isothiocyanate on Escherichia coli O157:H7 in refrigerated ground beef. *J. Food Prot.* **2003,** *66* (11), 2038-44.

15. Bertin, Y.; Habouzit, C.; Dunière, L.; Laurier, M.; Durand, A.; Duchez, D.; Segura, A.; Thévenot-Sergentet, D.; Baruzzi, F.; Chaucheyras-Durand, F.; Forano, E., Lactobacillus reuteri suppresses E. coli O157:H7 in bovine ruminal fluid: Toward a pre-slaughter strategy to improve food safety? *PLoS One* **2017,** *12* (11), e0187229.

16. Xie, W.; Song, L.; Wang, X.; Xu, Y.; Liu, Z.; Zhao, D.; Wang, S.; Fan, X.; Wang, Z.; Gao, C.; Wang, X.; Wang, L.; Qiao, X.; Zhou, H.; Cui, W.; Jiang, Y.; Li, Y.; Tang, L., A bovine lactoferricin-lactoferrampin-encoding Lactobacillus reuteri CO21 regulates the intestinal mucosal immunity and enhances the protection of piglets against enterotoxigenic Escherichia coli K88 challenge. *Gut Microbes* **2021,** *13* (1), 1956281.

17. Gao, J.; Cao, S.; Xiao, H.; Hu, S.; Yao, K.; Huang, K.; Jiang, Z.; Wang, L., Lactobacillus reuteri 1 Enhances Intestinal Epithelial Barrier Function and Alleviates the Inflammatory Response Induced by Enterotoxigenic Escherichia coli K88 via Suppressing the MLCK Signaling Pathway in IPEC-J2 Cells. *Front. Immunol.* **2022,** *13*, 897395.

18. Zhang, W.; Wang, H.; Liu, J.; Zhao, Y.; Gao, K.; Zhang, J., Adhesive ability means inhibition activities for lactobacillus against pathogens and S-layer protein plays an important role in adhesion. *Anaerobe* **2013,** *22*, 97-103.

19. Zhu, T.; Mao, J.; Zhong, Y.; Huang, C.; Deng, Z.; Cui, Y.; Liu, J.; Wang, H., L. reuteri ZJ617 inhibits inflammatory and autophagy signaling pathways in gut-liver axis in piglet induced by lipopolysaccharide. *J Anim Sci Biotechnol* **2021,** *12* (1), 110.

20. Cui, Y.; Liu, L.; Dou, X.; Wang, C.; Zhang, W.; Gao, K.; Liu, J.; Wang, H., Lactobacillus reuteri ZJ617 maintains intestinal integrity via regulating tight junction, autophagy and apoptosis in mice challenged with lipopolysaccharide. *Oncotarget* **2017,** *8* (44), 77489-77499.

21. Riva, A.; Kuzyk, O.; Forsberg, E.; Siuzdak, G.; Pfann, C.; Herbold, C.; Daims, H.; Loy, A.; Warth, B.; Berry, D., A fiber-deprived diet disturbs the fine-scale spatial architecture of the murine colon microbiome. *Nat Commun* **2019,** *10* (1), 4366.

22. Takahashi, S.; Tomita, J.; Nishioka, K.; Hisada, T.; Nishijima, M., Development of a prokaryotic universal primer for simultaneous analysis of Bacteria and Archaea using next-generation sequencing. *PLoS One* **2014,** *9* (8), e105592.

23. Douglas, G. M.; Maffei, V. J.; Zaneveld, J. R.; Yurgel, S. N.; Brown, J. R.; Taylor, C. M.;

Downloaded from https://www.cambridge.org/core. 07 Feb 2025 at 10:21:54, subject to the Cambridge Core terms of use.

Huttenhower, C.; Langille, M. G. I., PICRUSt2 for prediction of metagenome functions. *Nat Biotechnol* **2020,** *38* (6), 685-688.
24. Bolger, A. M.; Lohse, M.; Usadel, B., Trimmomatic: a flexible trimmer for Illumina sequence data. *Bioinformatics* **2014,** *30* (15), 2114-20.
25. Simpson, J. T.; Wong, K.; Jackman, S. D.; Schein, J. E.; Jones, S. J.; Birol, I., ABySS: a parallel assembler for short read sequence data. *Genome Res.* **2009,** *19* (6), 1117-23.
26. Blin, K.; Shaw, S.; Augustijn, H. E.; Reitz, Z. L.; Biermann, F.; Alanjary, M.; Fetter, A.; Terlouw, B. R.; Metcalf, W. W.; Helfrich, E. J. N.; van Wezel, G. P.; Medema, M. H.; Weber, T., antiSMASH 7.0: new and improved predictions for detection, regulation, chemical structures and visualisation. *Nucleic Acids Res* **2023,** *51* (W1), W46-w50.
27. Kautsar, S. A.; Blin, K.; Shaw, S.; Navarro-Muñoz, J. C.; Terlouw, B. R.; van der Hooft, J. J. J.; van Santen, J. A.; Tracanna, V.; Suarez Duran, H. G.; Pascal Andreu, V.; Selem-Mojica, N.; Alanjary, M.; Robinson, S. L.; Lund, G.; Epstein, S. C.; Sisto, A. C.; Charkoudian, L. K.; Collemare, J.; Linington, R. G.; Weber, T.; Medema, M. H., MIBiG 2.0: a repository for biosynthetic gene clusters of known function. *Nucleic Acids Res* **2020,** *48* (D1), D454-d458.
28. Agus, A.; Denizot, J.; Thévenot, J.; Martinez-Medina, M.; Massier, S.; Sauvanet, P.; Bernalier-Donadille, A.; Denis, S.; Hofman, P.; Bonnet, R.; Billard, E.; Barnich, N., Western diet induces a shift in microbiota composition enhancing susceptibility to Adherent-Invasive E. coli infection and intestinal inflammation. *Sci. Rep.* **2016,** *6*, 19032.
29. Martinez-Medina, M.; Denizot, J.; Dreux, N.; Robin, F.; Billard, E.; Bonnet, R.; Darfeuille-Michaud, A.; Barnich, N., Western diet induces dysbiosis with increased E coli in CEABAC10 mice, alters host barrier function favouring AIEC colonisation. *Gut* **2014,** *63* (1), 116-24.
30. Li, X.; Huang, G.; Zhang, Y.; Ren, Y.; Zhang, R.; Zhu, W.; Yu, K., Succinate signaling attenuates high-fat diet-induced metabolic disturbance and intestinal barrier dysfunction. *Pharmacol. Res.* **2023,** *194*, 106865.
31. Ghosh, S.; Nag, M.; Lahiri, D.; Sarkar, T.; Pati, S.; Kari, Z. A.; Nirmal, N. P.; Edinur, H. A.; Ray, R. R., Engineered Biofilm: Innovative Nextgen Strategy for Quality Enhancement of Fermented Foods. *Front Nutr* **2022,** *9*, 808630.
32. Liu, L.; Wu, R.; Zhang, J.; Li, P., Overexpression of luxS Promotes Stress Resistance and Biofilm Formation of Lactobacillus paraplantarum L-ZS9 by Regulating the Expression of Multiple Genes. *Front. Microbiol.* **2018,** *9*, 2628.
33. Speranza, B.; Liso, A.; Russo, V.; Corbo, M. R., Evaluation of the Potential of Biofilm Formation of Bifidobacterium longum subsp. infantis and Lactobacillus reuteri as Competitive Biocontrol Agents Against Pathogenic and Food Spoilage Bacteria. *Microorganisms* **2020,** *8* (2).
34. Lin, Y.; Chen, J.; Zhou, X.; Li, Y., Inhibition of Streptococcus mutans biofilm formation by strategies targeting the metabolism of exopolysaccharides. *Crit Rev Microbiol* **2021,** *47* (5), 667-677.
35. Deng, Z.; Hou, K.; Valencak, T. G.; Luo, X. M.; Liu, J.; Wang, H., AI-2/LuxS Quorum Sensing System Promotes Biofilm Formation of Lactobacillus rhamnosus GG and Enhances the Resistance to Enterotoxigenic Escherichia coli in Germ-Free Zebrafish. *Microbiol Spectr* **2022,** *10* (4), e0061022.
36. Liu, Z.; Zhang, Z.; Qiu, L.; Zhang, F.; Xu, X.; Wei, H.; Tao, X., Characterization and bioactivities of the exopolysaccharide from a probiotic strain of Lactobacillus plantarum WLPL04. *J Dairy Sci* **2017,** *100* (9), 6895-6905.
37. Ma, L.; Xu, X.; Peng, Q.; Yang, S.; Zhang, Y.; Tian, D.; Shi, L.; Qiao, Y.; Shi, B., Exopolysaccharide from Lactobacillus casei NA-2 attenuates Escherichia coli O157:H7 surface

Downloaded from https://www.cambridge.org/core. 07 Feb 2025 at 10:21:54, subject to the Cambridge Core terms of use.

adhesion via modulation of membrane surface properties and adhesion-related gene expression. *Microb. Pathog.* **2022,** *173* (Pt A), 105863.

38. Jelcić, I.; Hüfner, E.; Schmidt, H.; Hertel, C., Repression of the locus of the enterocyte effacement-encoded regulator of gene transcription of Escherichia coli O157:H7 by Lactobacillus reuteri culture supernatants is LuxS and strain dependent. *Appl Environ Microbiol* **2008,** *74* (10), 3310-4.

39. Montgomery, T. L.; Eckstrom, K.; Lile, K. H.; Caldwell, S.; Heney, E. R.; Lahue, K. G.; D'Alessandro, A.; Wargo, M. J.; Krementsov, D. N., Lactobacillus reuteri tryptophan metabolism promotes host susceptibility to CNS autoimmunity. *Microbiome* **2022,** *10* (1), 198.

40. Zhang, Y.; Tu, S.; Ji, X.; Wu, J.; Meng, J.; Gao, J.; Shao, X.; Shi, S.; Wang, G.; Qiu, J.; Zhang, Z.; Hua, C.; Zhang, Z.; Chen, S.; Zhang, L.; Zhu, S. J., Dubosiella newyorkensis modulates immune tolerance in colitis via the L-lysine-activated AhR-IDO1-Kyn pathway. *Nat Commun* **2024,** *15* (1), 1333.

41. Ognik, K.; Konieczka, P.; Mikulski, D.; Jankowski, J., The effect of different dietary ratios of lysine and arginine in diets with high or low methionine levels on oxidative and epigenetic DNA damage, the gene expression of tight junction proteins and selected metabolic parameters in Clostridium perfringens-challenged turkeys. *Vet Res* **2020,** *51* (1), 50.

42. Cheng, H.; Liu, J.; Zhang, D.; Wang, J.; Tan, Y.; Feng, W.; Peng, C., Ginsenoside Rg1 Alleviates Acute Ulcerative Colitis by Modulating Gut Microbiota and Microbial Tryptophan Metabolism. *Front. Immunol.* **2022,** *13*, 817600.

43. Bender, M. J.; McPherson, A. C.; Phelps, C. M.; Pandey, S. P.; Laughlin, C. R.; Shapira, J. H.; Medina Sanchez, L.; Rana, M.; Richie, T. G.; Mims, T. S.; Gocher-Demske, A. M.; Cervantes-Barragan, L.; Mullett, S. J.; Gelhaus, S. L.; Bruno, T. C.; Cannon, N.; McCulloch, J. A.; Vignali, D. A. A.; Hinterleitner, R.; Joglekar, A. V.; Pierre, J. F.; Lee, S. T. M.; Davar, D.; Zarour, H. M.; Meisel, M., Dietary tryptophan metabolite released by intratumoral Lactobacillus reuteri facilitates immune checkpoint inhibitor treatment. *Cell* **2023,** *186* (9), 1846-1862.e26.

44. Zhao, C.; Hu, X.; Bao, L.; Wu, K.; Feng, L.; Qiu, M.; Hao, H.; Fu, Y.; Zhang, N., Aryl hydrocarbon receptor activation by Lactobacillus reuteri tryptophan metabolism alleviates Escherichia coli-induced mastitis in mice. *PLoS Pathog.* **2021,** *17* (7), e1009774.

45. Li, J.; Zhang, L.; Wu, T.; Li, Y.; Zhou, X.; Ruan, Z., Indole-3-propionic Acid Improved the Intestinal Barrier by Enhancing Epithelial Barrier and Mucus Barrier. *J Agric Food Chem* **2021,** *69* (5), 1487-1495.

46. Dong, X. Y.; Azzam, M. M. M.; Zou, X. T., Effects of dietary threonine supplementation on intestinal barrier function and gut microbiota of laying hens. *Poult Sci* **2017,** *96* (10), 3654-3663.

47. Koo, B.; Choi, J.; Yang, C.; Nyachoti, C. M., Diet complexity and l-threonine supplementation: effects on growth performance, immune response, intestinal barrier function, and microbial metabolites in nursery pigs. *J Anim Sci* **2020,** *98* (5).

48. Cheng, M. J.; Wu, M. D.; Chen, J. J.; Su, Y. S.; Kuo, Y. H., Secondary Metabolites with Antimycobacterial Activities from One Actinobacteria: Herbidospora yilanensis. *Molecules* **2021,** *26* (20).

49. Xiao, J.; Zhang, Q.; Gao, Y. Q.; Tang, J. J.; Zhang, A. L.; Gao, J. M., Secondary metabolites from the endophytic Botryosphaeria dothidea of Melia azedarach and their antifungal, antibacterial, antioxidant, and cytotoxic activities. *J Agric Food Chem* **2014,** *62* (16), 3584-90.

50. Cui, Y.; Qi, S.; Zhang, W.; Mao, J.; Tang, R.; Wang, C.; Liu, J.; Luo, X. M.; Wang, H.,

Downloaded from https://www.cambridge.org/core. 07 Feb 2025 at 10:21:54, subject to the Cambridge Core terms of use.

Lactobacillus reuteri ZJ617 Culture Supernatant Attenuates Acute Liver Injury Induced in Mice by Lipopolysaccharide. *J Nutr* **2019,** *149* (11), 2046-2055.

51. Geraldo, B. M. C.; Batalha, M. N.; Milhan, N. V. M.; Rossoni, R. D.; Scorzoni, L.; Anbinder, A. L., Heat-killed Lactobacillus reuteri and cell-free culture supernatant have similar effects to viable probiotics during interaction with Porphyromonas gingivalis. *J. Periodontal Res.* **2020,** *55* (2), 215-220.

52. Özçam, M.; Tocmo, R.; Oh, J. H.; Afrazi, A.; Mezrich, J. D.; Roos, S.; Claesen, J.; van Pijkeren, J. P., Gut Symbionts Lactobacillus reuteri R2lc and 2010 Encode a Polyketide Synthase Cluster That Activates the Mammalian Aryl Hydrocarbon Receptor. *Appl Environ Microbiol* **2019,** *85* (10).

53. Liu, Z.; Zhang, Z.; Chen, X.; Ma, P.; Peng, Y.; Li, X., Citrate and hydroxycinnamate derivatives from Mume Fructus protect LPS-injured intestinal epithelial cells by regulating the FAK/PI3K/AKT signaling pathway. *J. Ethnopharmacol.* **2023,** *301*, 115834.

54. Vo, V. A.; Lee, J. W.; Shin, S. Y.; Kwon, J. H.; Lee, H. J.; Kim, S. S.; Kwon, Y. S.; Chun, W., Methyl p-Hydroxycinnamate Suppresses Lipopolysaccharide-Induced Inflammatory Responses through Akt Phosphorylation in RAW264.7 Cells. *Biomol. Ther. (Seoul)* **2014,** *22* (1), 10-6.

55. Li, Y. Y.; Wang, X. J.; Su, Y. L.; Wang, Q.; Huang, S. W.; Pan, Z. F.; Chen, Y. P.; Liang, J. J.; Zhang, M. L.; Xie, X. Q.; Wu, Z. Y.; Chen, J. Y.; Zhou, L.; Luo, X., Baicalein ameliorates ulcerative colitis by improving intestinal epithelial barrier via AhR/IL-22 pathway in ILC3s. *Acta Pharmacol Sin* **2022,** *43* (6), 1495-1507.

56. Ganapathy, A. S.; Saha, K.; Wang, A.; Arumugam, P.; Dharmaprakash, V.; Yochum, G.; Koltun, W.; Nighot, M.; Perdew, G.; Thompson, T. A.; Ma, T.; Nighot, P., Alpha-tocopherylquinone differentially modulates claudins to enhance intestinal epithelial tight junction barrier via AhR and Nrf2 pathways. *Cell Rep.* **2023,** *42* (7), 112705.

57. Liu, C.; Liu, J.; Wang, W.; Yang, M.; Chi, K.; Xu, Y.; Guo, N., Epigallocatechin Gallate Alleviates Staphylococcal Enterotoxin A-Induced Intestinal Barrier Damage by Regulating Gut Microbiota and Inhibiting the TLR4-NF-κB/MAPKs-NLRP3 Inflammatory Cascade. *J Agric Food Chem* **2023,** *71* (43), 16286-16302.

58. Zuo, G.; Chen, M.; Zuo, Y.; Liu, F.; Yang, Y.; Li, J.; Zhou, X.; Li, M.; Huang, J. A.; Liu, Z.; Lin, Y., Tea Polyphenol Epigallocatechin Gallate Protects Against Nonalcoholic Fatty Liver Disease and Associated Endotoxemia in Rats via Modulating Gut Microbiota Dysbiosis and Alleviating Intestinal Barrier Dysfunction and Related Inflammation. *J Agric Food Chem* **2024**.

59. Wu, Z.; Shen, J.; Xu, Q.; Xiang, Q.; Chen, Y.; Lv, L.; Zheng, B.; Wang, Q.; Wang, S.; Li, L., Epigallocatechin-3-Gallate Improves Intestinal Gut Microbiota Homeostasis and Ameliorates Clostridioides difficile Infection. *Nutrients* **2022,** *14* (18).

60. Ward, J. B. J.; Lajczak, N. K.; Kelly, O. B.; O'Dwyer, A. M.; Giddam, A. K.; J, N. G.; Franco, P.; Tambuwala, M. M.; Jefferies, C. A.; Keely, S.; Roda, A.; Keely, S. J., Ursodeoxycholic acid and lithocholic acid exert anti-inflammatory actions in the colon. *Am J Physiol Gastrointest Liver Physiol* **2017,** *312* (6), G550-g558.

61. Wang, G.; Fan, Y.; Zhang, G.; Cai, S.; Ma, Y.; Yang, L.; Wang, Y.; Yu, H.; Qiao, S.; Zeng, X., Microbiota-derived indoles alleviate intestinal inflammation and modulate microbiome by microbial cross-feeding. *Microbiome* **2024,** *12* (1), 59.

62. Coyte, K. Z.; Schluter, J.; Foster, K. R., The ecology of the microbiome: Networks, competition, and stability. *Science* **2015,** *350* (6261), 663-6.

63. Mazmanian, S. K.; Round, J. L.; Kasper, D. L., A microbial symbiosis factor prevents intestinal

Downloaded from https://www.cambridge.org/core. 07 Feb 2025 at 10:21:54, subject to the Cambridge Core terms of use.

inflammatory disease. *Nature* **2008,** *453* (7195), 620-5.
64. Lee, Y. K.; Mazmanian, S. K., Has the microbiota played a critical role in the evolution of the adaptive immune system? *Science* **2010,** *330* (6012), 1768-73.
65. Khafipour, E.; Krause, D. O.; Plaizier, J. C., A grain-based subacute ruminal acidosis challenge causes translocation of lipopolysaccharide and triggers inflammation. *J Dairy Sci* **2009,** *92* (3), 1060-70.
66. Yang, J.; Wei, H.; Zhou, Y.; Szeto, C. H.; Li, C.; Lin, Y.; Coker, O. O.; Lau, H. C. H.; Chan, A. W. H.; Sung, J. J. Y.; Yu, J., High-Fat Diet Promotes Colorectal Tumorigenesis Through Modulating Gut Microbiota and Metabolites. *Gastroenterology* **2022,** *162* (1), 135-149.e2.
67. Chassaing, B.; Koren, O.; Goodrich, J. K.; Poole, A. C.; Srinivasan, S.; Ley, R. E.; Gewirtz, A. T., Dietary emulsifiers impact the mouse gut microbiota promoting colitis and metabolic syndrome. *Nature* **2015,** *519* (7541), 92-6.

Figure legends

Figure 1. The characterization of *L. reuteri* ZJ617.

The representative SEM-images of *L. reuteri* ZJ617. The scale bar of left is 5 μm, the right is 1 μm.

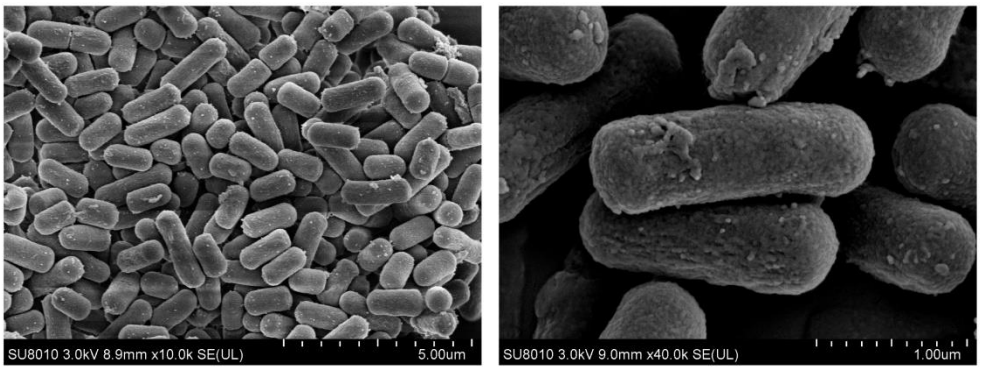

Downloaded from https://www.cambridge.org/core. 07 Feb 2025 at 10:21:54, subject to the Cambridge Core terms of use.

Figure 2. Genome information of *L. reuteri* ZJ617.

(A) Circular genomic map of *L. reuteri* ZJ617 chromosome and two plasmids. From the outermost to innermost circle, Circle 1 represents genome size; Circles 2 and 3 are forwards CDSs and reverse CDSs, respectively, color-coded according to the COG classification; Circles 4 is rRNA genes and tRNA genes; Circles 5 represents GC content; Circles 6 is GC skew. (B) The bar of KEGG pathway. (C) Threonine and L-Lysine biosynthesis pathway. (D) The secondary metabolite BGCs. (E) The classification of GCFs.

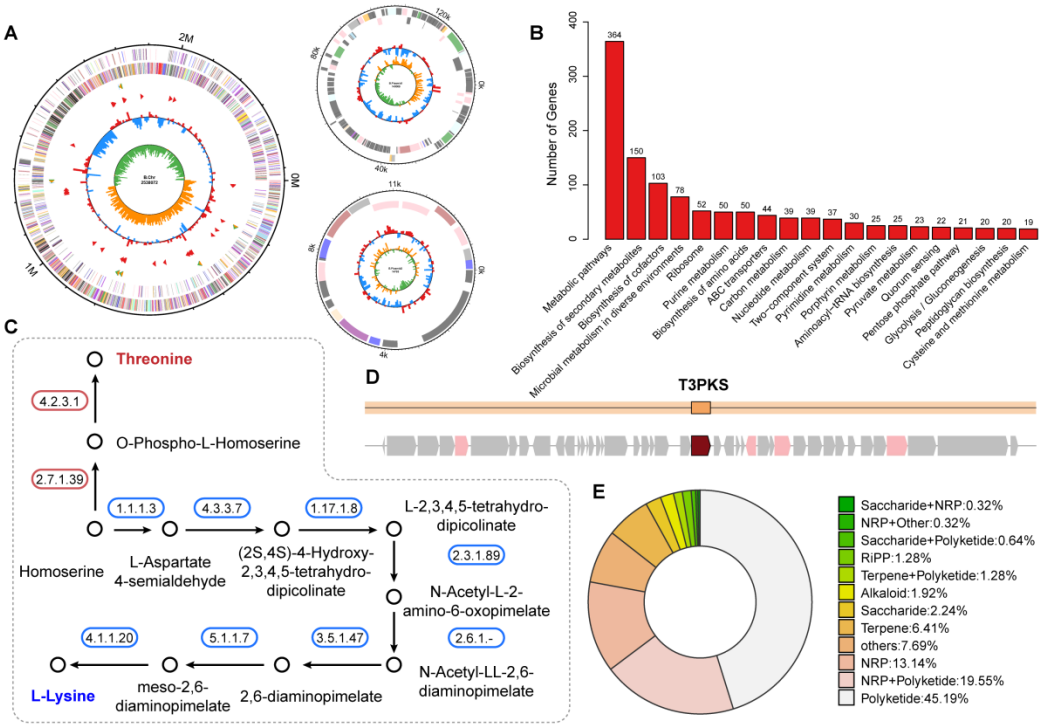

Downloaded from https://www.cambridge.org/core. 07 Feb 2025 at 10:21:54, subject to the Cambridge Core terms of use.

Figure 3. Metabolic pattern of *L. reuteri* ZJ617.

(A) PLS-DA score plot for discriminating the metabolic profile of *L. reuteri* ZJ617 before and after culture. (B) Volcano plots of significant changed metabolites of *L. reuteri* ZJ617 before and after culture. (C) The detected classification of metabolites. (D) The enriched KEGG pathway. (E) Heatmap of significant changed amino acids metabolites of *L. reuteri* ZJ617 before and after culture. (F) The part of significantly up-regulated secondary metabolites.

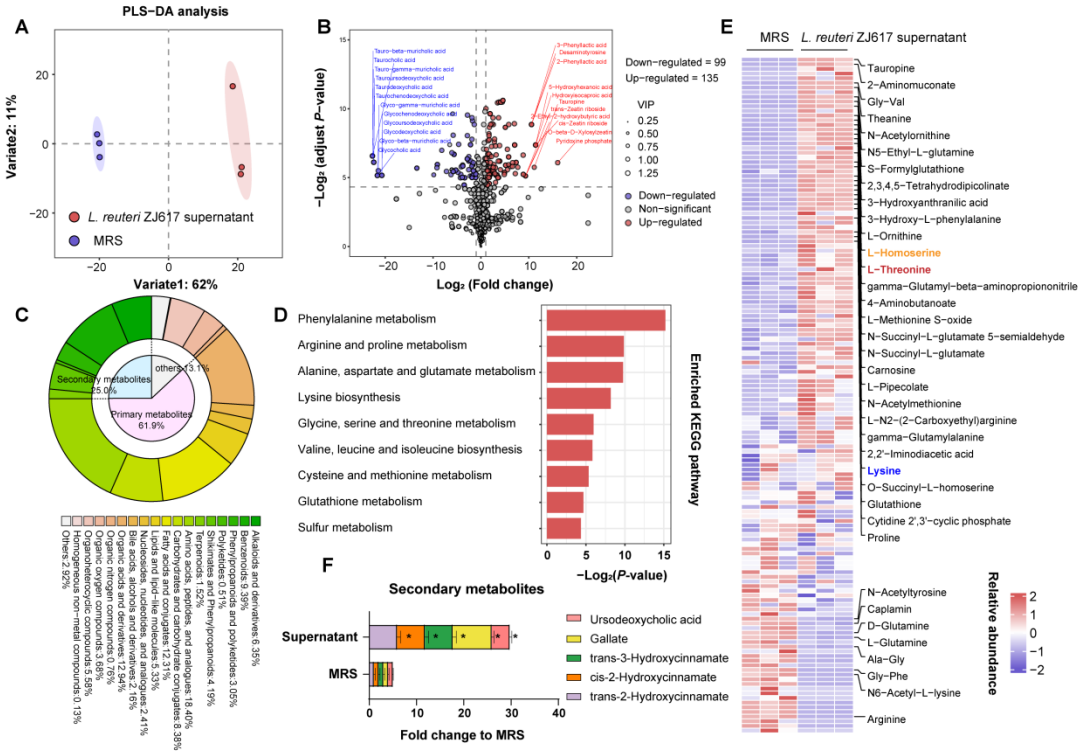

Downloaded from https://www.cambridge.org/core. 07 Feb 2025 at 10:21:54, subject to the Cambridge Core terms of use.

Figure 4. *L. reuteri* ZJ617 prevents obese mice from *E. coli*-induced serum inflammation

(A) Study design of *L. reuteri* ZJ617 intervention experiment. Mice were randomly assigned to three groups. After a week of adaption, all mice were fed with a high-fat diet, HZE mice were additionally supplemented with *L. reuteri* ZJ617 for 14 weeks. Two days before sacrifice, a half of HFD mice and all obese mice supplemented with *L. reuteri* ZJ617 were challenged with *E. coli* for 48h. (B) Body weight (g). (C-E) Serum inflammation index, including IL-1β, TNF-α and endotoxin.

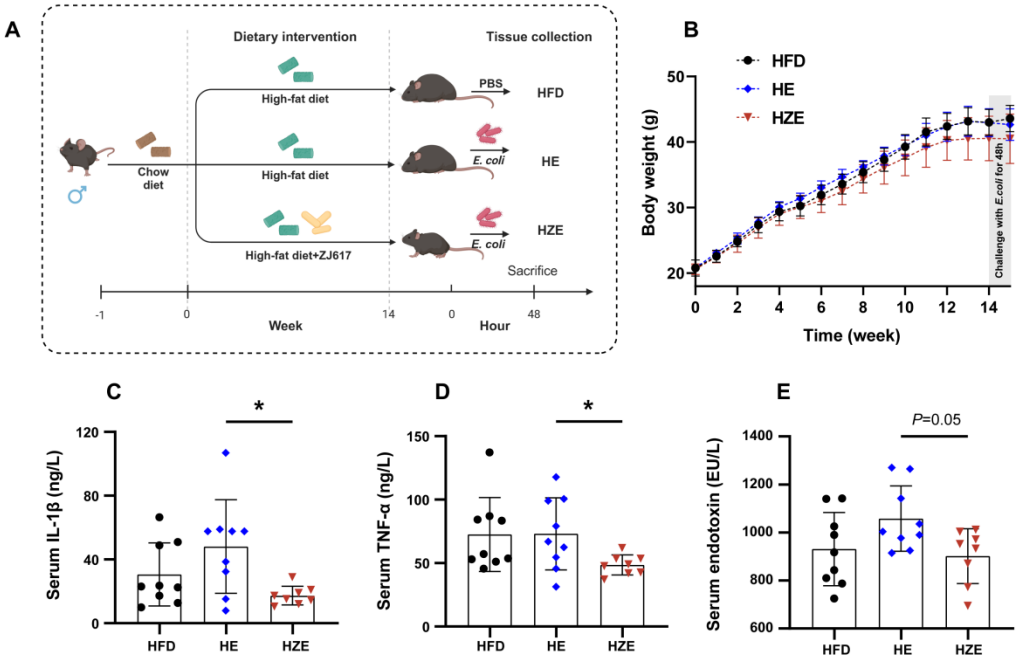

Downloaded from https://www.cambridge.org/core. 07 Feb 2025 at 10:21:54, subject to the Cambridge Core terms of use.

Figure 5. *L. reuteri* ZJ617 attenuates obese mice from *E. coli*-induced intestinal barrier damages

(A-B) Representative H&E images, villus height, crypt depth and their ration of ileum and colon, respectively (Scale bars, 500 μm). (C) Representative images of AB-stained colonic sections and mucus secretion (%) (Scale bars, 500 μm). (D-E) Protein level of ZO-1 and Occludin.

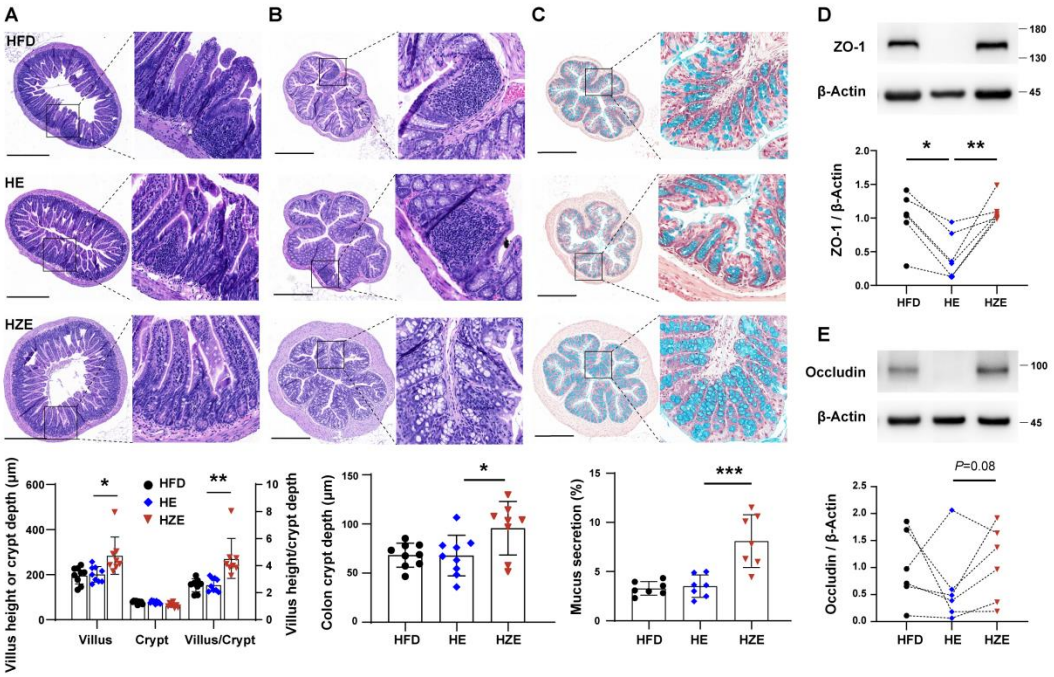

Figure 6. *L. reuteri* ZJ617 induces alterations in gut microbiome structure and functions

(A) Venn diagram. (B) chao1 index. (C) Unweighted UniFrac PCoA analysis of gut microbiota. (D) Relative abundance. (E-G) co-occurrence network of HFD, HE and HZE, respectively. (H) Degree. (I) clustering coefficient. (J) Bar chart represents functional pathways in intestinal contents predicted using PICRUSt2.

Downloaded from https://www.cambridge.org/core. 07 Feb 2025 at 10:21:54, subject to the Cambridge Core terms of use.

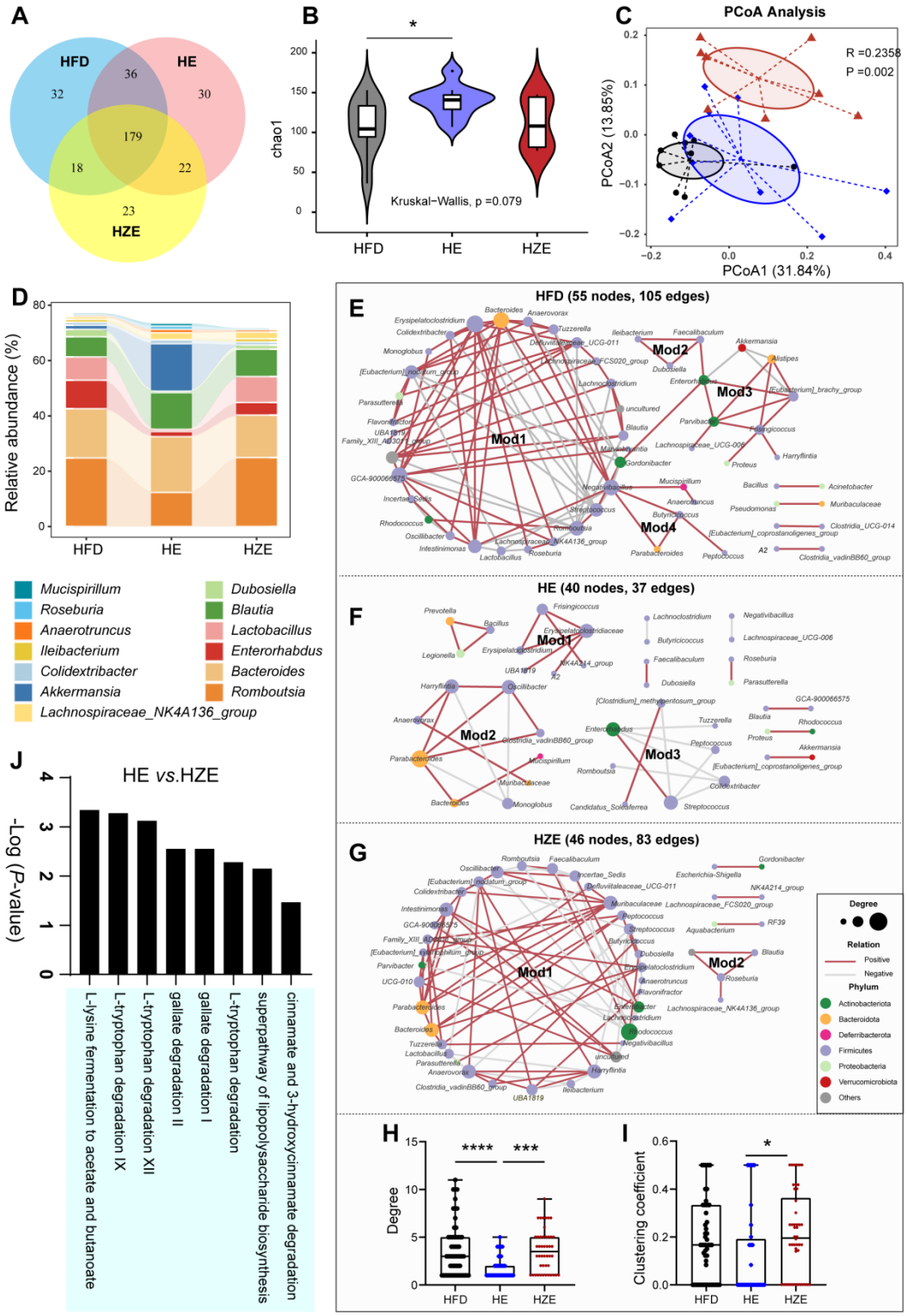

Downloaded from https://www.cambridge.org/core. 07 Feb 2025 at 10:21:54, subject to the Cambridge Core terms of use.

Figure S1. Metabolic classification of *L. reuteri* ZJ617.

The distribution of different types of metabolites in up-regulated and down-regulated states is shown. The Sankey diagram displays the up-regulated and down-regulated metabolites. Pie charts shows the percentage of each metabolite type in the total number of up-regulated or down-regulated metabolites.

Downloaded from https://www.cambridge.org/core. 07 Feb 2025 at 10:21:54, subject to the Cambridge Core terms of use.